

Conjugated polymer aggregates in solution: Control of interchain interactions

Thuc-Quyen Nguyen, Vinh Doan, and Benjamin J. Schwartz^{a)}

Department of Chemistry and Biochemistry, University of California, Los Angeles, Los Angeles, California 90095-1569

(Received 22 September 1998; accepted 17 November 1998)

We present evidence that the degree of interchain interactions and morphology in conjugated polymer films can be controlled by altering the chain conformation in the solution from which the film is cast. Light scattering experiments show that the physical size of poly[2-methoxy-5-(2'-ethyl-hexyloxy)-1,4-phenylene vinylene] (MEH-PPV) chains can vary by a factor of 2 in different solvents such as chlorobenzene (CB) or tetrahydrofuran (THF). Photoluminescence and wavelength-dependent excitation indicate that MEH-PPV forms aggregate species with an absorption and luminescence spectra that are distinctly red-shifted from the intrachain exciton. The degree of aggregation is both concentration and solvent dependent; for solutions with concentrations typical of those used in spin casting, aggregates comprise a significant fraction of the total number of excited state species. The overall photoluminescence quantum yield is found to depend both on how restricted the polymer conformation is due to the choice of solvent and on aggregation due to polymer concentration. The excited state aggregates have a longer lifetime than their intrachain exciton counterparts, as evidenced by a near-infrared transient absorption in femtosecond pump-probe and anisotropy measurements. Memory of the chain conformation and the extent of aggregation of MEH-PPV in solution is carried into cast films. Thus, many conflicting results presented on the degree of interchain interactions can be explained by noting that the film samples in different studies were cast from precursor solutions with different solvents and concentrations. Overall, a careful choice of the solution (both solvent and concentration) can be used to produce MEH-PPV films with desired interchain interactions for particular device applications. © 1999 American Institute of Physics. [S0021-9606(99)50408-X]

I. INTRODUCTION

Poly(*para*-phenylene vinylene) (PPV) and its derivatives are widely studied due to their semiconducting and luminescent properties. Within the class of PPVs, poly[2-methoxy-5-(2'-ethyl-hexyloxy)-1,4-phenylene vinylene] (MEH-PPV) exhibits characteristics that make it particularly favorable for device fabrication. In addition to preventing crystallization of the polymer when cast into films, the asymmetric alkoxy side chains (see the inset to Fig. 1 for a chemical structure) give MEH-PPV solubility in common organic solvents, allowing the use of processing techniques such as spin and drop casting.^{1,2} MEH-PPV also exhibits favorable charge injection properties in devices, with the valence band well matched to the work function of indium-tin-oxide (ITO) or poly(aniline) and the conduction band compatible with easily deposited metals such as aluminum or calcium.^{3,4} Despite these advantageous characteristics for device fabrication and a large number of photophysical studies, however, the nature of the excited states of PPVs, in general, and MEH-PPV, in particular, remains controversial.

One controversy with important implications for device performance focuses on whether the initial photoexcitation in PPVs produces only a single species. Several groups have observed that for PPV derivatives in dilute solutions when

the polymer chains are presumably isolated, the stimulated emission (SE), photoluminescence (PL), and photoinduced absorption (PA) decay dynamics are identical with a single characteristic relaxation time,⁵⁻⁹ typically ~300 ps. The natural assignment is that all these transient features result from a single excited state species, namely (intrachain) singlet excitons. In films of PPV derivatives, however, the PL yield is quenched relative to that in solution, and several groups have found that the SE dynamics differ from those of both the PL and the PA.^{6,9,10} Rothberg and co-workers have also reported that the PL in films of MEH-PPV has a small, long-lived tail.^{6,11} Moreover, these authors observed that the transient absorption dynamics varied with excitation wavelength: the PA increasingly overwhelms SE as the excitation wavelength is tuned to the blue.¹² These observations led Rothberg and co-workers to conclude that, in addition to excited intrachain excitons similar to those formed in solution, a new interchain electronic species is formed in the excited state in films. From their observations, these authors estimate that up to 90% of the species formed upon excitation of films are interchain.^{7,12}

In contrast, several groups have found evidence that photoexcitation in conjugated polymers produces mainly intrachain singlet excitons.¹³⁻¹⁶ Greenham *et al.* found a consistent relationship between the radiative lifetime, PL quantum yield, and PL decay time for films of several PPV

^{a)}Electronic mail: schwartz@chem.ucla.edu

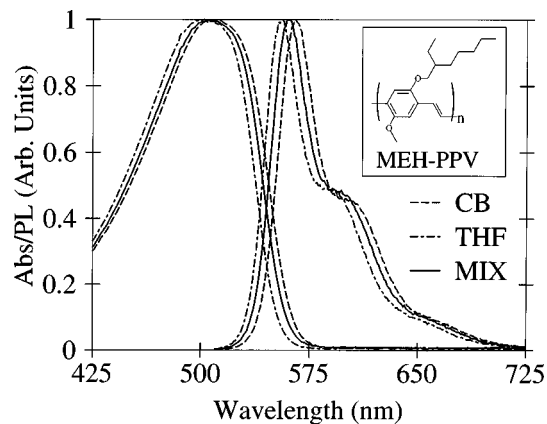


FIG. 1. Normalized absorption and PL spectra of MEH-PPV in dilute solutions of: chlorobenzene (CB, dashed curves); tetrahydrofuran (THF, dot-dashed curves), and a 1:1 mixture of CB:THF (mix, solid curves). Inset: Chemical structure of MEH-PPV.

derivatives, including MEH-PPV, leaving no room for significant branching to an interchain species.¹⁷ Vacar, Dogariu, and Heeger recently reexamined the excitation wavelength dependence of the photophysics of MEH-PPV films and found that the excited state properties were independent of the pump wavelength,¹⁸ providing no evidence for interchain species. Other work examining the excited state photophysics in films of an oligomeric analog of MEH-PPV found that the SE and PA dynamics agreed well at low excitation intensities and disagreed only at high intensities, prompting the suggestion that interchain species are mediated by doubly excited states on single chain segments that occur only at high excitation densities.¹⁹

Though the formation of interchain excited states in MEH-PPV is still a subject of much discussion, there is clear evidence for interchain species in other conjugated polymers. Studies of ladder-type poly(*para*-phenylene) (L-PPP),^{20–22} poly(*para*-pyridyl vinylene) (PPyV),^{23,24} and polyfluorene (PF)²⁵ derivatives show strong evidence for aggregate formation in films. The aggregates are characterized by delocalization of the electronic wave function among two or more chains in both the ground and excited states. This leads to the appearance of a new absorption band in films of these materials that is red-shifted relative to that in solution;²⁵ excitation of this band produces a broad, featureless, and highly Stokes shifted emission.^{20,23} Time-resolved measurements show that new band has a longer radiative lifetime than the intrachain excitation, as expected for a transition involving wave functions that are delocalized over several chain segments.^{22,24} Finally, studies based on near-field scanning optical microscopy (NSOM) show that aggregate species are spatially localized and that their optical properties vary from location to location within the polymer film.^{24,26} All these results suggest that conjugated polymer chains can aggregate to form electronic species with ground and excited state properties distinct from that of an isolated polymer chain.

In addition to interchain species composed of aggregates, Samuel and co-workers have recently argued that the formation of emissive interchain excimers plays an important role in the photophysics of a cyano-substituted PPV

(CN-PPV).^{27,28} Their arguments are based on the fact that the emission band in the film is highly red-shifted, broader, and loses vibronic structure compared to that in solution while the ground state absorption spectrum remains essentially unchanged. This led these authors to attribute the observed emission to interchain excimers, which have excitation delocalized between chains only in the excited state, instead of aggregates, which have a distinct delocalized ground state. This assignment is also supported by quantum yield and lifetime measurements, which suggest that the radiative lifetime of the emitting species in films is an order of magnitude longer than that in solution, indicating that the film emission comes from an electronic entity distinct from the intrachain exciton.²⁸ On making a detailed comparison between the photophysics of MEH-PPV and CN-PPV,²⁷ these authors note that like CN-PPV, (1) MEH-PPV shows a red-shift of its emission spectrum in the film compared to solution, although the band does not broaden or lose vibronic structure to the same degree as for CN-PPV; and (2) at low-excitation intensities, the emission lifetime of MEH-PPV films is longer than that in solution. Based on these observations, Samuel *et al.* suggest that MEH-PPV also forms interchain excimers in its excited state in films, but that the degree of excimer formation is intermediate between that of CN-PPV and unsubstituted PPV.²⁷

Rothberg and co-workers have recently revisited the photophysics of MEH-PPV films, and on the basis of the temperature dependence of the long-lived PL tail have concluded that the interchain species are excimers,¹¹ revising their original assignment of spatially indirect excitons or interchain polaron pairs.^{6,7,12,29} Thermal activation of interchain polaron pairs, which consist of a Coulombically bound electron and hole on physically adjacent chain segments, would be expected to cause charge transfer between chains to reform emissive intrachain excitons. Instead, the long-lived PL tail, which has a spectrum distinctly red-shifted from that of the intrachain exciton, is observed to increase markedly upon cooling.¹¹ These observations are readily explained if the interchain species is a weakly emissive excimer whose PL quantum yield is expected to drop as the temperature is increased due to an increase in the nonradiative relaxation rate.^{11,30–32}

The whole controversy over interchain excited states in polymers like MEH-PPV is especially important to consider when fabricating devices; the formation of weakly emissive interchain species would serve to significantly reduce the efficiency of electroluminescent conjugated polymer devices. Several groups have proposed solutions to reduce interchain coupling in conjugated polymers such as the use of extremely bulky side groups on the PPV backbone.^{33,34} This type of approach has the disadvantage, however, of also reducing the coupling needed to allow carriers to easily pass between chains; as a result, the improvement in luminescence efficiency in such materials is usually offset by poorer charge transport, as will be discussed further below. Thus, understanding and ultimately controlling interchain species remains a key challenge to optimize the efficiency of PPV polymers for use in electroluminescent devices.

In this paper, we present a new approach to controlling

the degree of interchain interactions in conjugated polymers: modifying the chain packing in the film by altering the chain morphology in the solution from which the film is cast. In the fabrication of conjugated polymer devices, polymers are often cast from solutions with very high concentrations, on the order of 1% weight/volume (w/v). We will show that the degree of interchain interaction and aggregation of MEH-PPV is directly related to both the concentration of polymer in the solution and the choice of solvent. Moreover, preliminary evidence suggests that the "memory" of the solution phase conformation is retained through the spin-casting process, resulting in solution-phase control over the morphology and photophysics of conjugated polymer films.

It is worth pointing out that the idea of interchain interactions of conjugated polymers in solution is not entirely new. For example, at concentrations significantly below those used in spin coating, the luminescence of poly(paraphenylene-2,6-benzobisoxazole) is strongly quenched in solutions due to excimer formation.³⁵ Moreover, Samuel and co-workers have recently shown that excimers of CN-PPV also form in solution, and that by varying the polarity of the solvent, the degree of excimer formation changed markedly.³⁶ The amount of excimerlike emission was highest in the poorest (most polar) solvents for CN-PPV, suggesting that this polymer tends to assemble in configurations favorable for excimer formation in these solvents. In this paper, we will show that the opposite is true for MEH-PPV: there is increased evidence for aggregate formation in nonpolar solvents and less so in poorer, more polar solvents.

As we will discuss below, some of the controversy that exists in the literature can be reconciled by the idea that the conformation of polymer chains in solution can influence the morphology and hence the interchain photophysics in films cast from different solvents. For example, MEH-PPV films prepared layer by layer using Langmuir-Blodgett techniques show significant differences in their photophysics from spin-cast films.³⁷ In addition, some work has found only photoinduced absorption (PA) at all probe wavelengths and no sign of stimulated emission (SE) or gain in MEH-PPV films cast from CB.^{6,7} On the other hand, SE has been observed in MEH-PPV films cast from tetrahydrofuran (THF), and, moreover, no pump wavelength dependence is observed for films cast from this solvent.¹⁸ The presence of SE in films cast from THF but not CB is also consistent with the fact that gain narrowing of the emission has been observed to occur in MEH-PPV films cast from THF pumped at high intensity, but that no narrowing is observed from CB-cast films.^{38,39} We will show that these observations are consistent with the extent of aggregation of MEH-PPV in the precursor solutions from which the films are cast.

In this paper, we present evidence of the concentration-dependent formation of weakly emissive aggregates of MEH-PPV in solution. Light scattering experiments show that the polymer takes a different conformation in different solvents, leading directly to differences in the photophysics as measured by UV-visible absorption and fluorescence spectroscopies. The emission quantum yield in solution also depends strongly on the choice of solvent. Fluorescence excitation spectra are found to vary with the choice of detection

wavelength, and show a distinct low-energy absorption responsible for emission at red wavelengths. Moreover, this low-energy peak shifts dramatically both with the polymer concentration and choice of solvent, providing evidence for MEH-PPV aggregates in solution. Finally, femtosecond pump and probe measurements show that different fractions of intrachain excitons and aggregates can be excited at different wavelengths, and that the presence of aggregates can be probed by PA at 800 nm. Anisotropy measurements show that excitations on aggregates are much less mobile than their intrachain counterparts. All these results suggest that the method by which conjugated polymer films are cast can at least partly control the interchain photophysics and, ultimately, the behavior of such films in electroluminescent devices.

II. EXPERIMENT

The MEH-PPV used in all the experiments performed here came from a single batch synthesized following the standard literature procedure.^{1,2} The molecular weight of the polymer was determined to be 535 000 g/mol by gel permeation chromatography (GPC). Sample solutions in chlorobenzene, tetrahydrofuran or a 50:50 (volume:volume) mix of the two solvents were prepared by dissolving the appropriate amount of polymer into the measured solvent and stirring for several hours. Solutions were stored in sealed vials in an inert atmosphere in the dark when not in use, and freshly dissolved solutions were used whenever possible. All the experiments reported here were performed at room temperature.

Light scattering measurements were performed on a Microtrac Ultrafine Particle Analyzer (Leeds & Northrup). The instrument makes use of a 780 nm diode laser, well to the red of the MEH-PPV absorption band, and measures the spectrum of frequency shifts of the scattered light. This allows the velocity or diffusion constant distribution of the polymer molecules to be directly inferred with standard analysis.⁴⁰ Using literature values for the viscosities of the solvents at room temperature and assuming that the laws of hydrodynamics are obeyed, the measured diffusion constants can be converted to a size distribution. The instrument is capable of distinguishing particles as small as 3 nm at relatively high particle concentrations.

UV-visible absorption spectra were recorded on a HP 8453 spectrophotometer using tungsten and deuterium lamps as light sources. The photoluminescence (PL) and photoluminescence excitation (PLE) spectra were measured on a Fluorolog-3 (Instrument S. A. & Co.) using a xenon lamp for the excitation source. PL quantum yield measurements were performed on this instrument using Rhodamine 101 in ethanol as a reference with an assumed quantum yield of unity.⁴¹ To minimize the effects of self-absorption, PL (and the emission in PLE) were collected from the front face of the sample for MEH-PPV solutions with concentrations $\geq 0.05\%$ w/v. At the highest concentrations, however, suppression of the PLE spectrum in the regions where the polymer most strongly absorbs indicated that self-absorption might be affecting the measured emission action spectra. Thus, to avoid distortions due to self-absorption, the PLE spectra presented

below in Fig. 4 are shown only where the optical density of the sample is less than 0.5. The presence of the below-gap bands in Fig. 4 in the absence of self-absorption was verified using very thin ($\leq 10 \mu\text{m}$) cells constructed by compressing a single drop of MEH-PPV solution between two microscope slides. The thin cells could not be used for quantitative work, however, because the cell thickness could not be reproducibly controlled and because solvent evaporation during cell fabrication altered the solution concentration.

Time-resolved SE and PA measurements were made using a regeneratively amplified Ti:Sapphire laser that produces ~ 120 fs light pulses centered at 800 nm with 1 mJ of energy at a 1 kHz repetition rate (Spectra Physics). These pulses pump a dual-pass optical parametric amplifier (OPA). For stimulated emission (SE) experiments, the OPA is set to produce signal and idler beams at 1350 and 1960 nm, respectively. The 1350 nm signal beam colinearly propagates with the residual 800 nm light into a type II BBO crystal to produce femtosecond pulses at 500 nm for excitation of MEH-PPV by sum-frequency mixing (SFM). The probe light at 585 nm is generated by SFM the residual 800 nm light from the first SFM process with the 1960 nm idler beam in a second, type I BBO crystal. For photoinduced absorption (PA) experiments, the OPA was tuned so that either the signal or idler beam had the correct wavelength for SFM with the residual 800 nm light to produce femtosecond pulses for exciting MEH-PPV samples at the desired wavelengths of 500, 575, or 592 nm, and the residual 800 nm light was used directly as the probe. All experiments on a particular polymer solution, including those with different pump or probe wavelengths, were performed on the same day to minimize the effects of degradation.

For all the femtosecond experiments, a small part of the probe light is split off to serve as a reference, and the remainder is attenuated with neutral density filters so that probe pulse energy at the sample is ≤ 50 nJ. A chopper mechanically modulates the pump beam at a frequency of ~ 280 Hz, and the difference signal between the probe and reference photodiodes is detected by lock-in amplification. The pump and probe beams are focused colinearly in the sample to a spot size of $\sim 200 \mu\text{m}$. The energy of the pump pulse and optical pathlength of the solutions were controlled to ensure that the excitation density in the sample did not exceed 10^{17}cm^{-3} ; thus, all the experiments reported here were below the excitation level where intensity-dependent effects such as exciton–exciton annihilation or amplified spontaneous emission are expected to occur.^{14,42–44} At these intensities, typical signal sizes were on the order of 1% change in optical density. The time delay between the pump and probe pulses is varied mechanically by a computer-controlled delay stage with $0.5 \mu\text{m}$ resolution.

Wave plates and polarizers are used to orient the polarization of the pump and probe beams with respect to each other. Unless otherwise specified, the relative polarization was set at the magic angle (54.7°) to prevent interference from dynamical processes that change the direction of the transition dipole of the species being probed.⁴⁵ Anisotropy measurements were made by first setting the relative polarizations of the pump and probe beams the same (\parallel), and then

repeating the measurement after rotating the probe polarization by 90° with respect to the pump (\perp). The anisotropy r is defined as⁴⁵

$$r = \frac{\parallel - \perp}{\parallel + 2\perp}.$$

The absolute magnitude of the measured polarized signal changes somewhat when changing polarization because many of the optics in the setup have polarization-dependent reflectivities. Thus, in the results presented below, the scans were scaled relative to one another to produce an anisotropy of 0.4 at time zero. When scaled this way, the linear combination $\parallel + 2\perp$ of the polarized scans decayed identically within the signal to noise of scans taken at the magic angle, verifying that our choice of scaling parameter is reasonable. The anisotropy observed for excitation into the main exciton absorption band is also consistent with that reported in previous work.¹⁰ In any event, as will be argued below, even if the absolute values of the anisotropy measured this way are subject to systematic error, it should not affect conclusions drawn from comparing the relative change in anisotropy loss between different scans treated in the identical way.

III. RESULTS AND DISCUSSION

We have elected to focus our attention on MEH-PPV because of both its widespread usage throughout the polymer community and, as discussed in the Introduction, the particular sensitivity of its photophysics to the local environment. Like most PPV derivatives, the essentially nonpolar MEH-PPV chains are readily soluble in aromatic solvents such as xylene or chlorobenzene (CB), and are still somewhat soluble in polar nonaromatic organic solvents like tetrahydrofuran (THF). To span the range of possible solution environments, we begin by examining the photophysics of MEH-PPV in CB, THF, and an equal volume mixture of the two solvents, hereafter referred to as the “mixed” solvent.

A. UV-visible absorption and PL. Basic photophysics of MEH-PPV in solution

The absorption and PL spectra of dilute (0.002% w/v) MEH-PPV solutions in THF, CB, and mixed solvent are shown in Fig. 1. The absorption and PL spectra of MEH-PPV are not the same in the three solvents: the absorption spectrum in CB is more red-shifted than that in THF, and the mixed solvent, not surprisingly, falls in between.

To explain the observed shifts by differential solvation of the ground and excited states would require that the polar solvent THF stabilize the nonpolar ground state of MEH-PPV better than the quinoid-like excited state: an idea that simply does not fit with the fact that THF is known to be a poor solvent for (ground state) MEH-PPV. The shifts can be explained, however, by considering that the conjugation length of the polymer changes in the different solvents. It is well known that the absorption band of oligomers shows a steady red-shift with an increasing conjugation length.⁴⁶ Studies have also shown that in conjugated polymers, including MEH-PPV,⁴⁷ the excitation energy tends to migrate to longer conjugation lengths before radiative relaxation, sometimes referred to as energy migration through the inhomoge-

neous density of states.^{48,49} Thus, a shorter average conjugation length for MEH-PPV in THF compared to CB not only explains the blue-shifted absorption spectrum, but also the blue-shifted emission.⁵⁰ In THF there must simply be fewer long conjugated segments for the energy to migrate to following excitation.

The differences created by the local solvent environment are also reflected in the PL quantum yield. We have measured the luminescence efficiency of MEH-PPV in dilute ($\leq 10^{-4}\%$ w/v) solutions of each of the three solvents, and find quantum yields of 0.39 ± 0.01 in CB; 0.27 ± 0.01 in THF; and 0.37 ± 0.03 in the mixed solvent. The measured efficiencies are relative to Rhodamine 101 as a standard (assumed quantum yield of unity),⁴¹ and the uncertainties are the standard deviation of three independent measurements in each solvent. The measured value in CB agrees well with previous quantum yield measurements of 0.35 for MEH-PPV in CHCl_3 and in the related aromatic solvent toluene,⁵¹ although another measurement has reported 0.20 in *p*-xylene.³³ Because the absolute quantum yields reported here were measured simply with a commercial instrument and not with an integrating sphere, they are likely subject to some degree of systematic error. All three solutions, however, were prepared and measured in the identical fashion, so that the relative quantum yields of MEH-PPV in the different solvents should be accurate. Thus, the most striking result is that the quantum efficiency of MEH-PPV in THF is only 70% that in CB.

The hypothesis of a shorter conjugation length in THF relative to CB also can be used to explain the relative quantum yields in the different solvents. MEH-PPV will tend to "unfold" in CB to maximize favorable π - π interactions between the polymer and the solvent, while the THF the polymer is expected to coil more tightly to minimize the number of aromatic repeat units interacting with the nonaromatic solvent molecules. The tighter polymer coil in THF would imply a greater number of torsional defects along the backbone and, hence, a lower PL quantum yield as well as a shorter conjugation length. The mixed solvent is expected to behave somewhat more like CB than THF since the polymer chains should be preferentially solvated by CB molecules. In the next section, we present physical evidence via light scattering that MEH-PPV indeed has significantly different conformations in different solvent environments.

B. Light scattering: The conformation of MEH-PPV in solution

We have performed light scattering experiments on MEH-PPV in different solutions in order to explore the idea of changing polymer conformation (and, hence, changing conjugation length) as the nature of the solvent is varied. By measuring the diffusion coefficient of the individual polymer chains and assuming the Stokes-Einstein relation, light scattering gives the size (hydrodynamic radius, R_H) distribution for the polymer chains. As expected, the experiments show that the conformation of MEH-PPV chains in solution is altered by the solvent-polymer interaction. Figure 2 shows typical light-scattering size distributions for the polymer chains in 0.5% w/v solutions of MEH-PPV in CB, THF, and

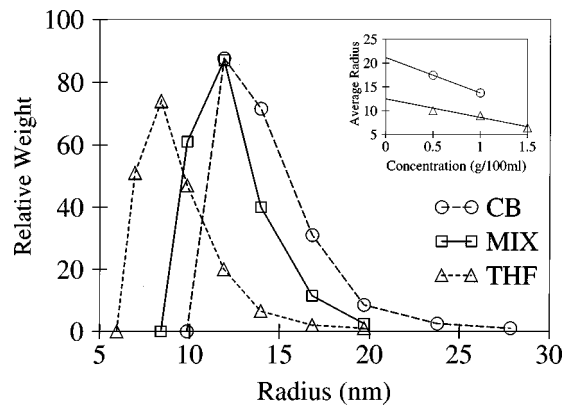


FIG. 2. Size distributions (hydrodynamic radii) from light scattering for solutions of MEH-PPV in: CB (circles); THF (triangles) and a 1:1 mix of CB:THF (squares). Lines connect the data points. Inset: The concentration dependence of average hydrodynamic radius; the symbols are the same as in the main figure.

the mixed solvent. It is clear that the average R_H in CB is nearly double that in THF and, as expected, the behavior in the mixed solvent is in between but closer to that of CB.

The inset of Fig. 2 shows the concentration dependence of R_H for MEH-PPV in CB and THF. The slight decrease in average R_H observed with an increasing concentration is likely due to multiple scattering. This is because an individual molecule has to diffuse much less distance to cause a change in the scattering signal when the light is multiply scattered. As a result, the scattering correlation function decays more quickly, leading to a higher apparent diffusion constant and thus a lower apparent R_H . In fact, as will be argued below, the polymer chains tend to aggregate with increasing concentration, so the apparent change in size with concentration represents a convolution of both multiple scattering and aggregation effects. We have studied the concentration dependence of the size distributions and extrapolated the average R_H values to zero concentration (Fig. 2, inset) to remove these effects. The result gives an average dilute solution R_H for MEH-PPV in CB of 21.5 nm, while that in THF is only 12.5 nm.

These numbers can be compared to previous work, which used both dynamic and angle-dependent light scattering to measure an R_H of 35.9 nm for MEH-PPV in *p*-xylene.³³ The difference between our results and those of Ref. 33 are likely due to both different polymer molecular weights (the 611 kg/mol for the polymer used in Ref. 33 should result in a larger coil than the 535 kg/mol used here), and differences in the solvents used (nonpolar *p*-xylene is a better solvent for MEH-PPV than the more polar CB). It is worth noting that obtaining absolute particle size measurements from nonmonodisperse samples is often tricky due to the mathematical deconvolution procedure involved in extracting the diffusion constant from the frequency shifts in the scattered light. However, all the samples we studied are from the same synthetic batch of polymer and were treated identically, so even if the results presented in Fig. 2 are subject to systematic error, it is still clear that the polymer conformation is significantly restricted in THF compared to CB. Overall, all the results argue that choice of solvent can be

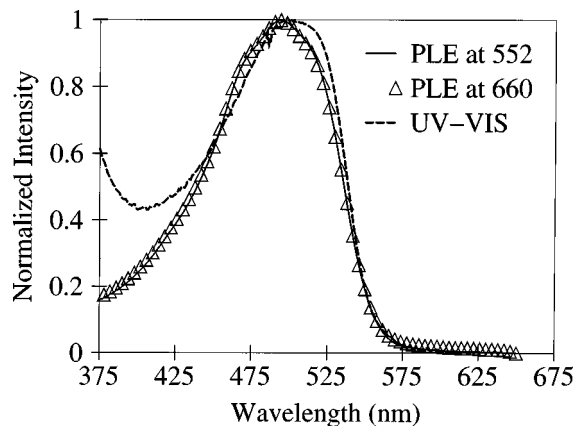


FIG. 3. Photoluminescence excitation spectra of MEH-PPV in a dilute THF solution for emission at 552 nm (a solid curve); 660 nm (triangles). The UV-visible absorption spectrum of the same solution is also shown for reference (dashed curve). The curves have been arbitrarily scaled for a best comparison.

used to systematically control the conformation of conjugated polymers.

C. Photoluminescence excitation: Evidence for aggregates

The effect of the solvent environment, and hence conformation of a polymer on its photophysics, can also be examined by photoluminescence excitation (PLE): scanning the excitation wavelength and collecting the amount of luminescence that results at a single chosen wavelength. For dilute MEH-PPV dissolved in CB, THF, and the mixed solvent, the PLE spectra that result from collecting emission near the band maximum at 552 nm resemble the standard absorption spectrum (Fig. 3). Like other groups, we observe some differences in the PLE and UV-visible spectra, most notably a decrease in the PLE relative to the absorption spectrum at blue wavelengths.^{10,11,33} The differences, however, are slight, making it difficult to argue their significance given that such differences may be sample dependent.^{11,13,17}

In Fig. 4, the below-gap PLE spectra of MEH-PPV solutions in THF at different concentrations are shown for detection at the red edge of the emission band (660 nm). As the concentration increases, a new excitation band appears to the red of the normal polymer absorption spectrum. This below-gap excitation feature increases in magnitude and red-shifts relative to the main absorption band with increasing concentration. This suggests that a large fraction of the emission at 660 nm is caused by a new species that has the bulk of its absorption spectrum to the red of the normal MEH-PPV absorption band. The observation of a new band that both absorbs and emits to the red of the polymer is similar to what is observed in L-PPP,^{20–22} PPyV,^{23,24} and PF²⁵ polymers, making it reasonable to assign the new feature in MEH-PPV to aggregates.

This assignment of the band observed in 660 nm PLE to aggregates is further confirmed by studying the concentration dependence. At very low concentrations (0.002% w/v), the 660 nm PLE is essentially identical to the 552 nm PLE, suggesting no significant aggregation (Fig. 3). The red-shift

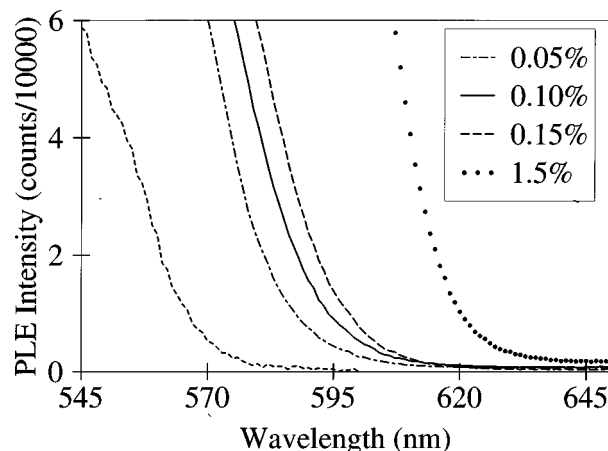


FIG. 4. The red onset of the 660 nm photoluminescence excitation for solutions of MEH-PPV in THF with different concentrations (w/v): 0.05% (dot-dashed curve); 0.1% (solid curve); 0.15% (long dashed curve); 1.5% (dots). The short-dashed curve shows the 552 nm PLE spectrum (which mirrors the UV-visible absorption) of the 1.5% solution for comparison.

and increasing relative intensity of the 660 nm PLE band (Fig. 4) suggest that both the size and number of aggregates grow with increasing concentration. As the MEH-PPV concentration is raised, aggregation provides more chain segments in contact over which the wave function can be delocalized, leading to both a redder ground state absorption and an increase in the total number of species that produce emission out in the red at 660 nm.

Figure 4 suggests that red emission from the aggregate species can be enhanced by preferentially exciting at the 660 nm PLE band maxima, an idea we will also return to when discussing the femtosecond pump-probe results in Sec. III D. The results of selective-excitation PL experiment are shown in Fig. 5, which compares the PL of MEH-PPV in a 1.5% w/v THF solution, excited at both 500 nm (the peak of main intrachain exciton absorption) and 592 nm (well into the aggregate band). The spike seen in the 592 nm excited scan is due to residual excitation light scattering into the PL collection monochromator of the fluorimeter. Excitation into the

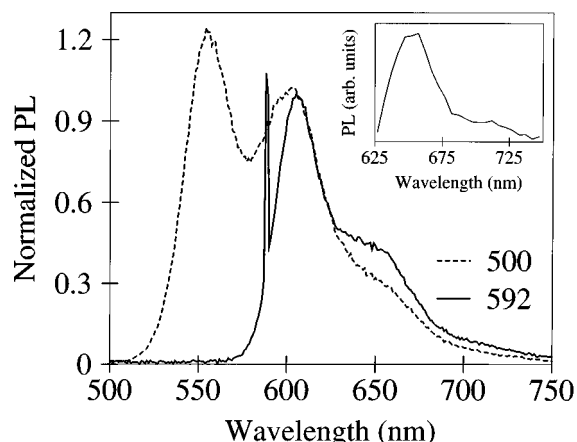


FIG. 5. Photoluminescence spectra of 1.5% w/v solutions of MEH-PPV in THF excited at 500 nm (dashed curve); 592 nm (solid curve). The spectra have been scaled to the same amplitude near 605 nm. Inset: The difference of the two spectra presented in the main figure.

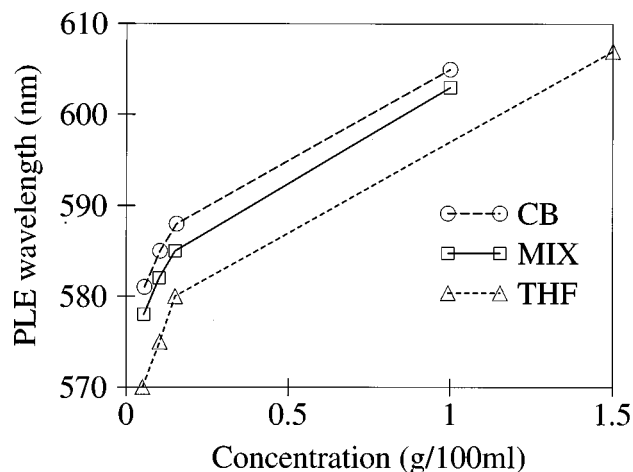


FIG. 6. The wavelength at which the 660 nm photoluminescence excitation spectra (Fig. 4) first rises to 60 000 counts as a function of concentration for MEH-PPV solutions of: CB (circles); THF (triangles); 1:1 CB:THF (squares). Lines connect the data points and are drawn to guide the eye.

aggregate band clearly increases the amount of PL in the red tail. The inset to Fig. 5 shows the results of scaling the two PL spectra for the best match at the $0 \rightarrow 1$ vibronic transition near 605 nm and then subtracting. The result is a broad, featureless band with a red tail that bears a striking resemblance to the aggregate emission seen in films of both other polymers^{20,23} and MEH-PPV.¹¹

To the best of our knowledge, Figs. 4 and 5 provide the first direct evidence for aggregate formation for MEH-PPV in solution. Unlike the previous studies that found aggregates in films in other polymers,^{20–25} in MEH-PPV solutions there is no distinct ground state absorption band nor obviously red-shifted emission to immediately point to aggregate formation.⁵⁰ The aggregate bands in solution show up in PLE, however, due to the fact that collection at red wavelengths is a more sensitive, aggregate-specific, zero-background technique compared to UV-visible absorption. It is also possible that the extent of wave function delocalization is different in solutions and films, leading to significantly lower oscillator strengths for the aggregate absorption and emission in solution.

Figure 6 provides evidence that the formation of MEH-PPV aggregates in solution can be controlled by the choice of solvent as well as the concentration. The aggregate excitation band shows a lower red-shift with increasing concentration in THF than in CB. From the light scattering results discussed above, we know that the polymer conformation is more open in CB than THF, providing both a higher number of longer conjugation length segments and increased access to those segments for promoting aggregation as the concentration is increased. This result also implies that the aggregate species are predominantly formed from conjugated segments on different chains; if aggregates were formed by a single chain folded back on itself, we would expect aggregate formation to be more facile in confining solvents like THF.

The fact that better solvents promote aggregation in MEH-PPV stands in contrast to previous work on CN-PPV, which found that interchain excimers form more readily in

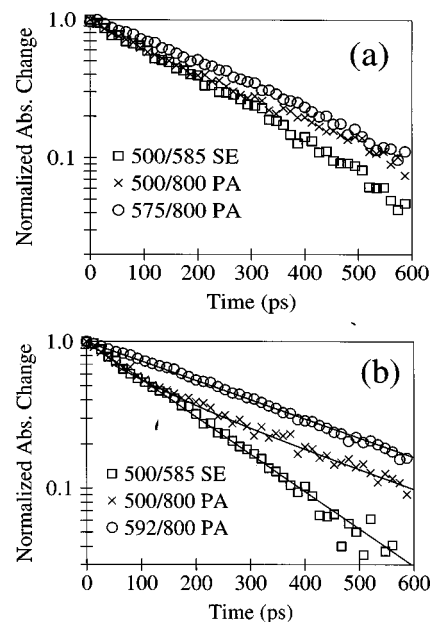


FIG. 7. Ultrafast pump-probe transients on 0.15% w/v (a) and 1.5% w/v (b) solutions of MEH-PPV in THF: 585 nm SE following 500 nm excitation (squares); 800 nm PA following 500 nm excitation (crosses); 800 nm PA following excitation at 575 nm (0.15% solution) or 592 nm (1.5% solution) (circles). The scans were arbitrarily scaled to the same magnitude at zero delay for a better comparison. The thin solid lines in (b) [not shown in (a) for clarity] are exponential fits to the data with parameters summarized in Table I.

poor solvents.³⁶ We suggest that the difference is due to the unique nature of the strongly electronegative cyano groups and symmetric substitution in CN-PPV that are known to cause strong interactions between chains in the film and likely promote efficient intrachain folding in solutions of unfavorable solvents. Clearly, the formation of interchain species in solutions of conjugated polymers depends on an interplay of factors including the nature of substituents on the polymer backbone as well as concentration and choice of solvent.

D. Femtosecond pump-probe spectroscopy: Excitons, aggregates, and conformation-dependent lifetimes

To further understand the behavior of MEH-PPV and its aggregates in solution, we have undertaken a series of femtosecond pump-probe experiments; typical results of these experiments (illustrated for MEH-PPV in THF solutions of two concentrations) are shown in Fig. 7, and the parameters for single or biexponential fits to these data are summarized in Table I.

The simplest of these experiments excites MEH-PPV in the center of its (intrachain) exciton absorption band at 500 nm and probes the change in sample absorbance at 585 nm as a function of the delay time. The 585 nm probe light is found to increase in intensity after passing through the excited sample; this negative change in absorbance is due to stimulated emission. By monitoring the decay of the stimulated emission signal with delay time (and assuming that other excited species do not absorb at the 585 nm probe wavelength), the lifetime of the emissive species can be mea-

TABLE I. Fit parameters for the pump-probe transients presented in Fig. 7 for solutions of MEH-PPV in THF: $a_1e^{-\tau_1} + a_2e^{-\tau_2}$ (see the text for details).

Concentration (% w/v)	$\lambda_{\text{pump}}/\lambda_{\text{probe}}$ (nm)	a_1	τ_1 (ps)	a_2	τ_2 (ps)
0.15	500/585 (SE)	1.000	201 ± 4		
1.5	500/585 (SE)	1.000	170 ± 3		
0.15	500/800 (PA)	0.468	273 ± 5	0.532	199 ± 4
1.5	500/800 (PA)	0.596	330 ± 3	0.404	118 ± 1
0.15	575/800 (PA)	1.000	273 ± 6		
1.5	592/800 (PA)	1.000	330 ± 3		

sured directly. Our initial measurements of this type started with dilute solutions of MEH-PPV in CB. We find the decay of the 585 nm SE signal fits well to a single exponential with a 301 ps lifetime, in excellent agreement with previous studies that measured ~ 300 ps excited state lifetimes in aromatic solutions by time correlated single photon counting,^{5,47,51} stimulated fluorescence depletion,⁶ or stimulated emission.¹⁰ We note that previous work has also examined solutions only at low ($<0.5\%$ w/v) concentrations.

The excited state dynamics of MEH-PPV in THF solutions, however, have a somewhat different behavior. Figure 7(a) presents the 500 nm pump/585 nm probe excited state decay for a 0.15% w/v solution of MEH-PPV in THF (squares). The SE signal decays single exponentially with a 201 ps lifetime. The measured decrease in lifetime between CB and THF solutions scales perfectly with the PL quantum yield measurements presented in Sec. III A; both measurements are consistent with a single radiative lifetime of ~ 0.8 ns, in reasonable agreement with previous estimates.^{17,47} The shorter SE lifetime in THF fits well with the concept of more tightly packed chains in THF compared to CB solutions. Excitons migrating along the chain in the restricted conformation in THF likely sample an increased number of defect sites leading to quenching of the luminescence.

In addition to a solvent dependence for the PL quantum yield and lifetime, we also have evidence for concentration quenching, presumably the result of aggregate formation, as discussed above. The squares in Fig. 7(b) show the SE decay in a 1.5% w/v solution of MEH-PPV in THF; here the solid line is a single exponential fit with a 170 ps time constant. The $\sim 15\%$ decrease in lifetime from (201–170 ps) upon increasing concentration (from 0.15% to 1.5%) suggests that even in THF solutions, which show a lower degree of aggregate formation compared to CB solutions (Fig. 6), when the concentration becomes comparable to that used in spin casting, aggregates comprise a significant fraction of the total number of excitations.

A direct probe of the role of aggregates in the excited state photophysics of MEH-PPV in solution is provided by experiments monitoring photoinduced absorption. Because intrachain excitons are known to have a strong PA in the near IR, in the absence of aggregates the kinetics measured for 800 nm PA should be identical to those measured for 585 nm SE. However, the 800 nm PA in MEH-PPV solutions following excitation at 500 nm shows two distinct time

scales: the expected decay that matches the exciton lifetime, as measured by SE at 585 nm, and a slower relaxation, which we assign as resulting from the decay of excited state aggregates (Fig. 7, crosses; Table I). In the 0.15% w/v THF solution, the slower 273 ps decay comprises a significant fraction of the observed 800 nm PA signal. Upon increasing the concentration to 1.5% w/v, the relative amplitude of the slower aggregate component increases and the decay time also increases slightly to 330 ps. The increased amplitude is consistent with a larger number of aggregates at the higher concentration, while the increased lifetime suggests the formation of larger aggregates with more delocalized wave functions (and therefore longer radiative lifetimes), consistent with the PLE results discussed above. Without knowing their relative excited-state absorption cross sections, it is difficult to determine exactly what fraction of the excited state species are intrachain excitons or aggregates. Since it is unlikely that the delocalized aggregate wave function has a significantly higher excited state absorption cross section than the intrachain exciton, Fig. 7 suggests that aggregates make up roughly tens of percents of the excited state population at high concentrations. The fact that aggregates comprise a significant fraction of the excited state species for 500 nm excitation implies that either the aggregates have a significant absorption under the main exciton absorption band (which was not evident in the PLE due to self-absorption), or that directly excited excitons can efficiently migrate to the sites of aggregation (in effect forming excimers).

One of the chief observations supporting the presence of interchain species in films has been a pump wavelength dependence to the PA dynamics. The idea is that excitation at different energies results in a different fraction of interchain species, leading to different kinetics of the PA.¹² For MEH-PPV solutions, the PLE results shown above suggest that aggregates can be preferentially excited to the red of the main exciton absorption. Thus, to verify our assignment of the long PA decay component as arising from aggregate states, we performed 800 nm transient absorption experiments pumping directly into the aggregate absorption bands (575 nm for the 0.15% solution and 592 nm for the 1.5% solution) of MEH-PPV in THF, shown as the circles in Fig. 7. Red excitation into the aggregate band clearly results in a longer PA decay (Fig. 7, circles) than excitation further to the blue into the exciton band (Fig. 7, crosses). The observed kinetics fit well to single exponentials, with lifetimes of 273 ps (0.15% solution) and 330 ps (1.5% solution), respectively, consistent with the idea that nearly all the species excited at these wavelengths are aggregates. Even more striking is the fact that at all concentrations, the observed kinetics match perfectly with the long decay component that resulted from 500 nm excitation (i.e., the long time tails of the two PA scans are parallel on the log plot of Fig. 7), suggesting that the decay is due to the same aggregate species in both cases.

As mentioned in the Introduction, Vacar, Dogariu, and Heeger recently have reported no pump wavelength dependence for the excited state dynamics in MEH-PPV solutions.¹⁸ In particular, they focused on $\sim 0.1\%$ w/v solutions of MEH-PPV in THF and chose 545 nm as one of their excitation wavelengths. Figures 4 and 5 suggest that 545 nm

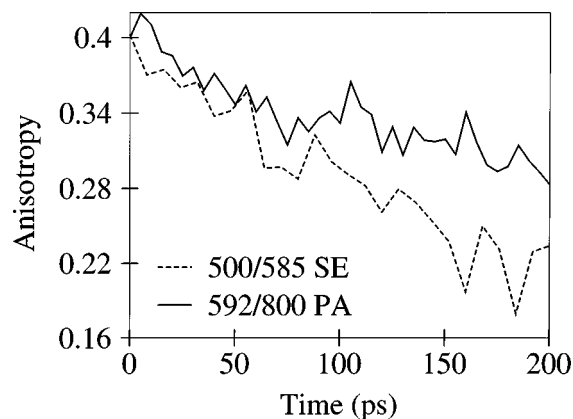


FIG. 8. Femtosecond transient anisotropy for 1.5% w/v solutions of MEH-PPV in THF: 585 nm SE produced by 500 nm excitation (dashed curve); 800 nm PA produced by 592 nm excitation (solid curve).

light can access the aggregate band absorption for MEH-PPV in THF at this concentration. Figure 7(a), however, implies that at low concentrations, the evidence for long-lived aggregates in PA does not appear until times ≥ 300 ps. None of the data reported in Ref. 18 shows times longer than 300 ps. The data shown in Fig. 7(a) agree well with the limited time range that is presented in Ref. 18; thus, this previous study may simply not have excited the dilute sample sufficiently to the red nor explored to long enough delay times to observe the subtle difference in PA due to aggregates in solution. Overall, Fig. 7 shows that with proper choice of excitation wavelength, solvent and concentration, control over the lifetimes of excitons, and aggregates, as well as their relative population, is possible.

Since the aggregate states are localized in space to regions where multiple chain segments are physically adjacent, time-resolved anisotropy can be used to provide further evidence that the long-lived species are aggregates. Energy transfer causes excitons to migrate along or between polymer chain segments which may have different orientations, resulting in a loss of anisotropy following the initial excitation.^{10,52,53} Because they are tied to a particular region in space, it is unlikely that there will be any significant motion of aggregate states, leading to the expectation of a slower loss of anisotropy for aggregates.

With the correct choice of pump and probe wavelengths, the anisotropy dynamics can be measured independently for both intrachain excitons and aggregates. Since the aggregate species emit further to the red than the intrachain excitons, 585 nm SE can be used to probe exclusively excitons. Conversely, excitation at 592 nm is well beyond the exciton absorption band, so the resulting PA probes predominantly aggregates. Figure 8 presents anisotropy decays for each of these cases in 1.5% w/v MEH-PPV in THF. The solid curve shows the anisotropy decay of the 800 nm aggregate PA produced by selectively pumping the aggregate band, while the dashed curve shows the anisotropy of the exciton SE probed at 585 nm. The anisotropy decay of the intrachain exciton is qualitatively consistent with that reported for 850 nm PA following 390 nm excitation in previous work.¹⁰ The results in Fig. 8 show that the PA anisotropy decays slower

than that of the SE, consistent with aggregate species that are less mobile than excitons.

E. Solution phase aggregates: Implications for interchain interactions in films

Unlike the results presented in Fig. 4, PLE studies on MEH-PPV films cast from THF¹¹ or other solvents⁵⁴ show little evidence for a band to the red of the main intrachain exciton absorption band. This could be due to a lack of aggregate species in films, or, more likely, results from quenching of the weak aggregate emission due to the increased number of pathways available for nonradiative relaxation in the solid state. The situation is further complicated by the fact that energy transfer is facile in conjugated polymer films.⁴⁹ Even if aggregation in the solid state is insufficient to result in a distinct ground state species, as argued above for solutions, migration of intrachain excitations could result in trapping at low-energy aggregate sites, essentially resulting in excimer formation^{21,30} (this process appears not to be important, however, for excimers of CN-PPV in solution³⁶). We note that whether they are produced by direct excitation or exciton migration, the branching ratio between any electronic species that are shared between several chain segments and intrachain excitons should be wavelength dependent. For the aggregate case, the aggregate absorption cross section will vary with wavelength in a different fashion than that of the intrachain exciton, resulting in different relative numbers of each for excitation at different wavelengths. For the excimer case, excitation at different wavelengths produces excitons of different mobility, altering the probability of diffusion to a site that facilitates sharing of the excitation energy between neighboring chains. In this section, we argue that aggregates in conjugated polymer solutions persist through the casting process, resulting in fundamental changes in the photophysical and electroluminescent behavior of conjugated polymers in the solid state.

The most compelling reason that solution-phase aggregates of conjugated polymers are important in the solid state is that most conjugated polymer films are cast from highly concentrated solutions: the same concentrations ($\sim 1\%$ w/v) at which aggregate formation was shown above to play an important role. Evidence that the chain packing in conjugated polymer films is controlled by the choice of polymer concentration in solution has already been provided by x-ray diffraction studies of polyaniline films.⁵⁵ Moreover, MEH-PPV films drop cast from CB and THF have been observed in recent work to have different local structures, showing that the choice of solvent affects film morphology.⁵⁶ Differing photophysics in films cast from different solvents, such as the presence of SE and line-narrowing in films of MEH-PPV cast from THF but not in films cast from CB, was pointed out in the Introduction and will be discussed further below. Finally, recent theoretical arguments³⁰⁻³² and experimental work^{27,28} suggest that excimer formation is indeed important in films of conjugated polymers and in MEH-PPV, in particular.¹¹

As argued above, MEH-PPV chains in CB solution take an open, extended conformation (Fig. 2) which, relative to THF solutions, tends to promote the formation of aggregates

in highly concentrated solutions (Fig. 6). Upon spin casting, the slow evaporation of the relatively high-boiling CB tends to preserve these interchain species: there is plenty of time for favorable interchain interactions to dominate the solid-state structure while the solvent evaporates. Thus, we can expect that MEH-PPV chains in films cast from CB tend to remain aggregated. Figure 7 demonstrates that aggregate states give rise to a PA; if this absorption extends to the blue of 800 nm into the emission region, the presence of aggregates will lower or possibly overwhelm the net cross section for SE, and thus the possibility for line narrowing in such films. This reasoning is consistent with the complete lack of SE^{6,7} and line narrowing³⁸ observed in CB-cast films of MEH-PPV.

MEH-PPV chains in THF solution, on the other hand, take a compact conformation (Fig. 2) and thus, relative to CB, tend to resist forming aggregates in highly concentrated solutions (Fig. 6). Upon spin casting, rapid evaporation of the volatile THF solvent tends to favor retention of the tightly coiled chains: there is simply too little time for chain–chain or substrate–chain interactions to cause the polymer to extend its conformation before the solvent has evaporated. Thus, we can expect that the MEH-PPV chains in films cast from THF are still tightly coiled, and that relative to films cast from CB, interchain aggregation is reduced. A lower number of aggregates in THF-cast films is consistent with pump wavelength-independent photophysics at early times,¹⁸ as discussed above. Moreover, reduced aggregation allows SE from intrachain excitons to more effectively compete with the PA from interchain species, consistent with the presence of SE¹⁸ and line narrowing³⁸ in THF (but not CB^{6,8}) cast films of MEH-PPV.

In addition to photophysics, the preservation of aggregates from solutions to films of conjugated polymers also has important implications for the operation of electroluminescent devices. The quenching of emission of intrachain excitons and the formation of aggregated traps is clearly detrimental to obtaining high luminescence efficiencies from light-emitting devices. In addition, the morphology of conjugated polymers in films can have a significant effect on charge transport.⁵⁵ For example, strong interchain interactions likely favor charge transport and thus could be beneficial for conjugated polymers in photovoltaic devices. Since it is unlikely that a single chain spans the two electrodes in a polymer-based device, reducing interchain interactions by casting films of MEH-PPV from THF rather than CB is expected to lead to poorer interchain charge transport and thus reduced carrier mobility. This idea is verified by the fact that LEDs produced from CB-cast films of MEH-PPV are known to have a lower turn-on voltage and higher working current than devices produced from THF-cast films.⁵⁷

Overall, the luminescent and charge transport properties of MEH-PPV films can be controlled by both the concentration and choice of solvent in the precursor solution. By careful choice of the casting conditions, it may be possible to optimize interchain interactions for both device performance and luminescence yield. For example, MEH-PPV films cast from *p*-xylene show line narrowing at high excitation intensities (although with a higher threshold than films cast from

THF)³⁸ and are also known to make good light-emitting devices. We are presently studying the photophysical properties of MEH-PPV films cast from solutions of different concentrations as well as from solvent mixtures in the search for ways to optimize the use of this material for particular applications.⁵⁴

IV. CONCLUSIONS

In summary, we have shown that the conformation of MEH-PPV varies greatly in different solvents. MEH-PPV chains in CB solution are much more extended and open than in THF solutions, as evidenced by (1) the size distributions measured directly by light scattering; (2) the red-shift of the UV-visible absorption and PL spectra in CB solutions relative to THF; and (3) the drop in luminescence quantum yield and exciton lifetime in THF solutions relative to CB. Moreover, the photophysics of MEH-PPV in solution are also seen to vary with concentration. PLE spectra for red emission wavelengths show a new band to the red of the intrachain exciton absorption, which is attributed to aggregates. The presence of aggregates is confirmed by a red-shift and rise in the intensity of this band along with a corresponding decrease in quantum yield upon increasing polymer concentration. The degree of aggregate formation is seen to be solvent dependent, with the open conformation of MEH-PPV in CB solutions allowing more efficient interchain coagulation than the tighter coil, which is prevalent in THF solutions, a result opposite that of previous studies on CN-PPV. Photoexcitation at different wavelengths results in a different fraction of excited intrachain excitons and interchain aggregate species, as confirmed by both CW and time-resolved spectroscopies. The presence of excited-state aggregates can be monitored directly with 800 nm transient absorption, and the inability of the aggregate wave function to migrate via energy transfer results in a slower anisotropy decay than that observed for intrachain excitons.

Preliminary evidence suggests that “memory” of the solution-phase conformation of MEH-PPV is retained through the casting process, so that the method by which polymers are cast results in control over the interchain interactions in the film. Thus, many of the conflicts in the literature concerning the photophysics of conjugated polymers are the result of studying samples that were cast from different solutions and therefore have different degrees of interchain coupling. The photophysics of MEH-PPV films cast from different solvents, for example, have markedly different photophysical properties, such as the ability for films cast from THF to undergo stimulated emission and line narrowing while films cast from CB cannot. The charge transport properties of MEH-PPV films cast from THF, however, are noticeably inferior to those of CB-cast films. With careful study, it should be possible to choose the solution (both solvent and concentration) that produces a film with the interchain interactions desired for a particular device application.

Note added in proof. We recently became aware of the related work of Gelinck, Staring, Warman, and co-workers [Synth. Met. **84**, 595 (1997); J. Phys. Chem. **100**, 5455 (1996)] who found aggregation effects in a broken-

conjugated alkoxy-substituted PPV derivative using microwave conductivity.

ACKNOWLEDGMENTS

We thank Roger Helgeson, Bin Ma, and Fred Wudl for providing the MEH-PPV used in this work as well as the apparatus for UV-visible absorption and fluorimetry measurements. We thank Fred Hawthorne and Andreas Maderna for the use of the particle sizing instrument, and Erik Barthel for assistance with the femtosecond pump-probe measurements. Acknowledgment is made to the donors of the Petroleum Research Fund, administered by the ACS, for partial support of this work (Grant No. 32773-G6). This work was also supported by setup funds from UCLA, and a grant from the UCLA Council on Research (4-563835-19914-07).

- ¹F. Wudl, P. M. Alleman, G. Srdanov, Z. Ni, and D. McBranch, ACS Symp. Ser., 455 (1991).
- ²F. Wudl and S. Hoger, PCT Patent Application WO 94/20589, 1991.
- ³G. Gustafsson, G. M. Treacy, Y. Cao, F. Klavetter, N. Colaneri, and A. J. Heeger, Nature (London) **357**, 477 (1992).
- ⁴G. Yu, Synth. Met. **80**, 143 (1996).
- ⁵L. Smilowitz, A. Hays, A. J. Heeger, G. Wang, and J. E. Bowers, J. Chem. Phys. **98**, 6504 (1993).
- ⁶M. Yan, L. J. Rothberg, E. W. Kwock, and T. M. Miller, Phys. Rev. Lett. **75**, 1992 (1995).
- ⁷J. M. Leng, S. Jeglinski, X. Wei, R. E. Brenner, and Z. V. Vardeny, Phys. Rev. Lett. **72**, 156 (1994).
- ⁸L. J. Rothberg, M. Yan, F. Papdimitrakopoulos, M. E. Galvin, E. W. Kwock, and T. M. Miller, Synth. Met. **80**, 41 (1996).
- ⁹B. J. Schwartz, F. Hide, M. R. Andersson, and A. J. Heeger, Chem. Phys. Lett. **265**, 327 (1997).
- ¹⁰J. Z. Zhang, M. A. Kreger, Q.-S. Hu, D. Vitharana, L. Pu, P. J. Brock, and J. C. Scott, J. Chem. Phys. **106**, 3710 (1997).
- ¹¹R. Jakubiak, L. J. Rothberg, W. Wan, and B. R. Hsieh, Synth. Met. (in press).
- ¹²M. Yan, L. J. Rothberg, F. Papdimitrakopoulos, M. E. Galvin, and T. M. Miller, Phys. Rev. Lett. **72**, 1104 (1994).
- ¹³N. T. Harrison, G. R. Hayes, R. T. Phillips, and R. H. Friend, Phys. Rev. Lett. **77**, 1881 (1996).
- ¹⁴G. J. Denton, N. Tessler, N. T. Harrison, and R. H. Friend, Phys. Rev. Lett. **78**, 733 (1997).
- ¹⁵S. V. Frolov, M. Liess, P. A. Lane, W. Gellermann, Z. V. Vardeny, M. Ozaki, and K. Yoshino, Phys. Rev. Lett. **78**, 4285 (1997).
- ¹⁶J. W. Blatchford, S. W. Jessen, L. B. Lin *et al.*, Phys. Rev. Lett. **76**, 1513 (1996).
- ¹⁷N. C. Greenham, I. D. W. Samuel, G. R. Hayes, R. T. Phillips, Y. A. R. R. Kessener, S. C. Moratii, A. B. Holmes, and R. H. Friend, Chem. Phys. Lett. **241**, 89 (1995).
- ¹⁸D. Vacar, A. Dogariu, and A. J. Heeger, Chem. Phys. Lett. **290**, 58 (1998).
- ¹⁹V. I. Klimov, D. W. McBranch, N. N. Barashkov, and J. P. Ferraris, Chem. Phys. Lett. **277**, 109 (1997).
- ²⁰U. Lemmer, S. Heun, R. F. Mahrt, U. Scherf, M. Hopmeier, U. Siegner, E. O. Göbel, K. Mahn, and H. Bassler, Chem. Phys. Lett. **240**, 373 (1995).
- ²¹T. Pauck, R. Hennig, M. Perner, U. Lemmer, U. Siegner, R. F. Mahrt, U. Scherf, K. Mullen, and H. Bassler, Chem. Phys. Lett. **244**, 171 (1995).
- ²²R. F. Mahrt, T. Pauck, U. Lemmer *et al.*, Phys. Rev. B **54**, 1759 (1996).
- ²³J. W. Blatchford, S. W. Jessen, L.-B. Lin *et al.*, Phys. Rev. B **54**, 9180 (1996).
- ²⁴J. W. Blatchford, T. L. Gustafson, A. J. Epstein *et al.*, Phys. Rev. B **54**, R3683 (1996).
- ²⁵M. Grell, D. D. C. Bradley, X. Long, T. Chamberlain, M. Inbasekaran, E. P. Woo, and M. Soliman, Acta Polym. **49**, 439 (1998).
- ²⁶J. A. DeAro, K. D. Weston, S. K. Buratto, and U. Lemmer, Chem. Phys. Lett. **277**, 532 (1997).
- ²⁷I. D. W. Samuel, G. Rumbles, and C. J. Collison, Phys. Rev. B **52**, R11 573 (1995).
- ²⁸I. D. W. Samuel, G. Rumbles, C. J. Collison, R. H. Friend, S. C. Moratii, and A. B. Holmes, Synth. Met. **84**, 497 (1997).
- ²⁹J. W. P. Hsu, M. Yan, T. M. Jedju, and L. J. Rothberg, Phys. Rev. B **49**, 712 (1994).
- ³⁰E. M. Conwell, Synth. Met. **85**, 995 (1997).
- ³¹E. M. Conwell, Phys. Rev. B **57**, 14 200 (1998).
- ³²M. W. Wu and E. M. Conwell, Phys. Rev. B **56**, R10 060 (1997).
- ³³C. L. Gettenger, A. J. Heeger, J. M. Drake, and D. J. Pine, J. Chem. Phys. **101**, 1673 (1994).
- ³⁴B. R. Hsieh, Y. Yu, E. W. Forsythe, G. M. Schaaf, and W. A. Feld, J. Am. Chem. Soc. **120**, 231 (1998).
- ³⁵S. A. Jenekhe and J. A. Osaheni, Science **265**, 765 (1994).
- ³⁶I. D. W. Samuel, G. Rumbles, C. J. Collison, S. C. Moratii, and A. B. Holmes, Chem. Phys. **227**, 75 (1998).
- ³⁷M. I. Sluch, C. Pearson, M. C. Petty, M. Halim, and I. D. W. Samuel, Synth. Met. **94**, 285 (1998).
- ³⁸F. Hide, M. A. Díaz-García, B. J. Schwartz, M. R. Andersson, Q. Pei, and A. J. Heeger, Science **273**, 1833 (1996).
- ³⁹W. Holzer, A. Penzkofer, S. H. Gong, D. D. C. Bradley, X. Long, and A. Bleyer, Chem. Phys. **224**, 315 (1997).
- ⁴⁰B. Berne and R. Pecora, *Dynamic Light Scattering with Applications to Chemistry, Biology, and Physics* (Wiley, New York, 1976).
- ⁴¹I. B. Berlman, *Handbook of Fluorescence Spectra of Aromatic Molecules*, 2nd ed. (Academic, New York, 1984).
- ⁴²R. G. Kepler, V. S. Valencia, S. J. Jacobs, and J. J. McNamara, Synth. Met. **78**, 227 (1996).
- ⁴³D. Vacar, A. Dogariu, and A. J. Heeger, Adv. Mater. **10**, 669 (1998).
- ⁴⁴V. Doan, V. Tran, and B. J. Schwartz, Chem. Phys. Lett. **228**, 576 (1998).
- ⁴⁵C. R. Cantor and P. R. Schimmel, *Biophysical Chemistry Part II* (Freeman, San Francisco, 1980), p. 454.
- ⁴⁶R. Kersting, U. Lemmer, R. F. Mahrt, K. Leo, H. Kurz, H. Bässler, and E. O. Göbel, Phys. Rev. Lett. **70**, 3820 (1993).
- ⁴⁷G. R. Hayes, I. D. W. Samuel, and R. T. Phillips, Phys. Rev. B **52**, R11 569 (1995).
- ⁴⁸Ch. Warmuth, A. Tortschanoff, K. Brunner, B. Mollay, and H. F. Kauffmann, J. Lumin. **76 & 77**, 498 (1998).
- ⁴⁹R. Kersting, B. Mollay, M. Rusch, J. Wenisch, G. Leising, and H. F. Kauffmann, J. Chem. Phys. **106**, 2850 (1997).
- ⁵⁰M. Zheng, F. Bai, and D. Zhu, J. Photochem. Photobiol., A **116**, 143 (1998).
- ⁵¹I. D. W. Samuel, B. Crystall, G. Rumbles, P. L. Burn, A. B. Holmes, and R. H. Friend, Chem. Phys. Lett. **213**, 472 (1993).
- ⁵²A. Watanabe, T. Kodaira, and O. Ito, Chem. Phys. Lett. **273**, 227 (1997).
- ⁵³G. R. Hayes, I. D. W. Samuel, and R. T. Phillips, Phys. Rev. B **56**, 3838 (1997).
- ⁵⁴V. Doan, T.-Q. Nguyen, and B. J. Schwartz (in preparation).
- ⁵⁵W. Zheng, M. Angelopoulos, A. J. Epstein, and A. G. MacDiarmid, Macromolecules **30**, 7634 (1997).
- ⁵⁶C. Y. Yang, F. Hide, M. A. Díaz-García, and A. J. Heeger, Polymer **39**, 2299 (1998).
- ⁵⁷Y. Yang (private communication).